Journal of Cellular Physiology

Y-Box binding protein-1 is part of a complex molecular network linking ΔNp63α to the PI3K/AKT pathway in cutaneous squamous cell carcinoma

Journal:	*Journal of Cellular Physiology*
Manuscript ID:	JCP-14-0704.R1
Wiley - Manuscript type:	Original Research Article
Date Submitted by the Author:	19-Dec-2014
Complete List of Authors:	Troiano, Annaelena; Università di Napoli Federico II, Dipartimento di Biologia Schiano Lomoriello, Irene; University Federico II, Biologia di Martino, Orsola; University Federico II, Biologia Fusco, Sabato; University of Naples, Center for Advanced Biomaterials for Health Care@CRIB, Istituto Italiano di Tecnologia, Naples, Italy. Pollice, Alessandra; University of Naples, Dipartimento di Biologia Vivo, Maria; University of Naples, Dipartimento di Biologia La Mantia, Girolama; University of Naples, Biologia Strutturale e Funzionale Calabro, Viola; University Federico II, Dipartimento di Biologia
Key Words:	p53 protein family, Y-box binding protein, PI3K/AKT/PTEN, cell proliferation, skin cancer

Y-Box binding protein-1 is part of a complex molecular network linking ΔNp63α to the PI3K/AKT pathway in cutaneous squamous cell carcinoma

Annaelena Troiano, Irene Schiano Lomoriello, Orsola di Martino, Sabato Fusco§, Alessandra Pollice, Maria Vivo, Girolama La Mantia, Viola Calabrò*

Department of Biology, University of Naples "Federico II", 80128 Naples, Italy

§Center for Advanced Biomaterials for Health Care@CRIB, Istituto Italiano di Tecnologia, Naples, Italy.

Running Title: YB-1, ΔNp63α and the PI3K pathway cross-talk

Keywords: **p53 protein family, Y-box binding protein, PI3K/AKT/PTEN, cell proliferation, squamous carcinoma, skin cancer**.

This work was supported by Progetto "Campania Research in Experimental Medicine" (CREME), POR Campania FSE 2007-2013 to V. C. and Regione Campania L R N°5/2007 to G. L. M.

Corresponding author: Prof. Viola Calabrò, PhD. Dipartimento di Biologia, Università di Napoli, "Federico II", Viale Cinzia, Monte S Angelo, 80126 Napoli, Italy. Phone: +39 081 679069. Fax +39 081 679033. E-mail: vcalabro@unina.it

Abstract

Cutaneous squamous cell carcinomas (SCCs) typically lack somatic oncogene-activating mutations and most of them contain p53 mutations. However, the presence of p53 mutations in skin premalignant lesions suggests that these represent early events during tumor progression and additional alterations may be required for SCC development. SCC cells frequently express high levels of ΔNp63α and Y-box binding 1 (YB-1 or YBX1) oncoproteins. Here, we show that knockdown of YB-1 in spontaneously immortalized HaCaT and non-metastatic SCC011 cells led to a dramatic decrease of ΔNp63α, cell detachment and death. In highly metastatic SCC022 cells, instead, YB-1 silencing induces PI3K/AKT signaling hyperactivation which counteracts the effect of YB-1 depletion and promotes cell survival. In summary, our results unveil a functional cross-talk between YB-1, ΔNp63α and the PI3K/AKT pathway critically governing survival of squamous carcinoma cells.

Introduction

Squamous cell carcinoma (SCC) is a treatment-refractory malignancy arising within the epithelium of different organs, that is frequently associated with overexpression of ΔNp63α oncoprotein (Rocco et al., 2006, Hibi et al., 2000). ΔNp63α is encoded by the TP63 locus, the ancestral gene of the p53 gene family that gives rise to multiple isoforms that can be placed in two categories: TA isoforms with an acidic transactivation domain and ΔN isoforms that lack this domain. Alternative splicing at the carboxy-terminal (C-terminal) generates at least three p63 variants (α, β and γ) in each class (Rossi et al., 2006, Yang et al., 1999). ΔNp63α is essential for the maintenance of the proliferative capacity of epithelial cell progenitors (Senoo et al., 2004); as these cells start to differentiate, ΔNp63α protein level gradually drops and those that no longer express ΔNp63α, loose the proliferative capacity (Koster, 2010).

In squamous carcinoma, ΔNp63α up-regulation causes skin hyperplasia and abnormal keratinocyte differentiation predisposing to malignant transformation (Hibi et al., 2000; Moll and Slade, 2004). Despite its undisputed relevance in epithelial cancer, the mechanisms through which ΔNp63α executes its pro-oncogenic functions are not fully understood. However, ΔNp63α expression was shown to be induced by activation of downstream targets of EGFR activation including STAT3 (Ripamonti et al., 2013) and the phosphoinositide-3-kinase (PI3K) pathway (Barbieri et al., 2003).

We have recently shown that ΔNp63α interacts with the YB-1 oncoprotein and promotes accumulation of YB-1 into the nuclear compartment (Di Costanzo et al., 2012; Amoresano et al., 2010). YB-1, also named YBX1, is a member of the cold shock domain (CSD) protein family, which is found in the cytoplasm and nucleus of mammalian cells, being able to shuttle between the two compartments (Eliseeva et al., 2011). The YB-1 gene, located on chromosome 1p34 (Toh et al., 1998), encodes a 43 kDa protein having three functional domains: a variable NH2-terminal Alanine/Proline rich tail domain (aa 1-51), involved in transcriptional regulation, a highly

conserved nucleic acid binding domain (CSD, aa 51-171), and a COOH-terminal tail (B/A repeat) for RNA/ssDNA binding and protein dimerization (129-324).

YB-1 is a major downstream target of Twist (Shiota et al., 2008) and c-Myc-Max complexes by recruitment to the E-box consensus sites in YB-1 promoter (Uramoto et al., 2002). YB-1 regulates genes promoting cancer cell growth such as EGFR, Her-2, PI3KCA and MET (To et al., 2010) as well as genes linked to cancer stem cells such as those encoding the hyaluronan receptor CD44, CD49f (integrin α6) and CD104 (β4 integrin), implying that YB-1 plays a key role as oncogene by transactivating genes associated with a cancer stem cell phenotype (To et al., 2010). YB-1 protein level drastically increases during progression of several types of tumors including squamous carcinoma, thereby suggesting a role for this protein in the pathogenesis of human epithelial malignancy (Di Costanzo et al., 2012, Kolk et al., 2011).

To mediate gene regulation, YB-1 translocates into the nucleus and interacts with the proximal promoter regions of its target genes (Sutherland et al., 2005; Shiota et al., 2011). Phosphorylation of serine 102 in response to MAPK and PI3K/AKT signaling promotes YB-1 nuclear translocation (Sinnberg et al., 2012). Moreover, YB-1 translocates to the nucleus when cells are exposed to cytokines, anticancer agents, hyperthermia, or UV light irradiation (Schittek et al., 2007).

Herein, we present data showing the existence of a functional cross-talk between YB-1, ΔNp63α and the PI3K/AKT signaling pathway critically governing survival of squamous carcinoma cells.

MATERIALS AND METHODS

Plasmids

The 1.1 Kb EGFR promoter luciferase plasmid was provided by Dr. A.C. Johnson (US National Cancer Institute, Massachusetts, USA). The cDNA encoding human ΔNp63α and ΔNp63α F518L were previously described (Lo Iacono et al., 2006).

Cell lines, transfection and antibodies

SCC011 and SCC022 cell lines were established from cutaneous squamous carcinomas (Lefort et al., 2007). SCC011 and SCC022 cells were cultured in RPMI supplemented with 10% fetal bovine serum at 37°C and 5% CO_2. HaCaT and MDA-MB231 cells were purchased from Cell Line Service (CLS, Germany) and cultured at 37°C and 5% CO_2. HaCaT cells were maintained in DMEM supplemented with 10% FBS. MDA-MB231 cells were maintained in DMEM supplemented with 5% FBS.

Transient transfection

Lipofections were performed with Lipofectammine 2000 (Life Technologies, CA, USA), according to the manufacturer's recommendations.

YB1 transient silencing was carried out with IBONI YB-1siRNA pool (RIBOXX GmbH, Germany) and RNAiMAX reagent (Life Technologies, CA, USA), according to the manufacturer's recommendations. Briefly, cells were seeded at 60% confluence (1.5×10^6) in 100-mm dishes and transiently silenced with IBONI YB1-siRNA at 20 nM final concentration.

YB-1 guide sequences:

UUUAUCUUCUUCAUUGCCGCCCCC;

UUAUUCUUCUUAUGGCAGCCCCC;

UUCAACAACAUCAAACUCCCCC;

UCAUAUUUCUUCUUGUUGGCCCCC.

ΔNp63α transient silencing was carried out with IBONI p63-siRNA pool (RIBOXX GmbH, Germany) at 20 nM final concentration and RNAiMAX reagent (Life Technologies, CA, USA).

p63 guide sequences:

UUAAACAAUACUCAAUGCCCCC;

UUAACAUUCAAUAUCCCACCCCC;

AUCAAUAACACGCUCACCCCC;

AUGAUUCCUAUUUACCCUGCCCCC.

"All Star Negative Control siRNA", provided by Quiagen (Hilden, Germany), was used as negative control.

Transfection efficiency of siRNA was quantified using BLOCK-iT™ Control Fluorescent Oligo (Life Technologies, CA, USA) at a final concentration of 20 nM using Lipofectamine RNAiMAX (Life Technologies, CA, USA). Cells were stained with Hoechst and transfected cells detected by direct immunofluorescence. Transfection efficiency ranged between 70 and 80% .The percentage of transfected cells was estimated as the average of counts performed on 100 cells in five independent fields.

Immunoblot analyses and coimmunoprecipitation

Immunoblots (IB) were performed as previously described (Di Costanzo et al., 2012). Briefly, 30 μg of whole cell extracts were separated by SDS-PAGE, subjected to immunoblot and incubated overnight at 4°C with antibodies.

For nuclear-cytoplasmic fractionation 10 μg of nuclear and 30 μg of cytoplasmic extracts (1:3 rate) were separated by SDS-PAGE and subjected to immunoblot.

All images were acquired with CHEMIDOC (Bio Rad, USA) and analyzed with the Quantity-ONE software.

Coimmunoprecipitation was performed as previously described (Rossi et al., 2006). Briefly, whole HaCaT cell extracts, precleared with 30 μl of protein A-agarose (50% slurry; Roche, Manheim,

Germany), were incubated overnight at 4°C with anti-p63 (2 µg) or α-mouse IgG. The reciprocal experiment was performed with anti-YB-1(3 µg) or α-rabbit IgG (3 µg).

Antibodies and chemical reagents

Anti-p63 (4A4), anti-cytokeratin 1 (4D12B3), anti-GAPDH (6C5), and anti-actin (1-19) were purchased from Santa Cruz (Biotechnology Inc. CA, USA). PARP, PTEN, AKT, pAKT ^{S473}, EGFR and STAT3 antibodies were from Cell Signaling Technology (Beverly, Massachusetts). Rabbit polyclonal YB1 (Ab12148) antibody was purchased from Abcam (Cambridge, UK). Proteasome inhibitor MG132 were purchased from Sigma-Aldrich (St Louis, MO) and used at 10 µM final concentration in DMSO (Sigma-Aldrich, St Louis, MO). LY294002 was purchased from Calbiochem (CA, USA) and used at 50 µM final concentration in DMSO.

Cell Viability assay

Cell viability was determined by the MTT 3-(4,5-dimethylthiazol-2-yl)-2,5-diphenyl tetrazolium bromide assay (Sigma-Aldrich, St Louis, MO). Briefly, cells were seeded in 96-well plates at 2 x 10^3 and transfected with scrambled or YB-1 siRNA oligos, 48h after silencing MTT solution (5mg/ml in PBS, 20 µl/well) was added to cells to produce formazan crystals. MTT solution was substituted by 150 µl DMSO 30 minutes later to solubilize the formazan crystals. The optical absorbance was determined at 570 nm using an iMark microplate reader (Bio-Rad, USA). The experiments were carried out in triplicate for each knockdown and compared to scrambled control (value set at 1.0).

Quantitative Real Time-PCR

For PCR analysis total RNA was isolated using the RNA Extraction Kit from Qiagen (Hilden, Germany) according to the manufacturer's instructions. RNA (2-5µg) was treated with DNAse I

(Promega, Madison USA) and used to generate reverse transcribed cDNA using SuperScript III (Life Technologies, CA, USA), according to the manufacturer's instructions. All samples in each experiment were reverse transcribed at the same time, the resulting cDNA diluted 1:5 in nuclease-free water and stored in aliquots at –80°C until used.

Real Time PCR with SYBR green detection was performed with a 7500 RT-PCR Thermo Cycler (Applied Biosystem, Foster City, USA). The thermal cycling conditions were composed of 50ºC for 2 min followed by an initial denaturation step at 95ºC for 10 min, 45 cycles at 95ºC for 30s, 60ºC for 30s and 72ºC for 30s. Experiments were carried out in triplicate. The relative quantification in gene expression was determined using the $2^{-\Delta\Delta Ct}$ method (Livak and Schmittgen, 2011). Using this method, we obtained the fold changes in gene expression normalized to an internal control gene and relative to one control sample (calibrator). 18S was used as an internal control to normalize all data and the siCtrl was chosen as the calibrator.

Appropriate no-RT and non-template controls were included in each 96-well PCR reaction and dissociation analysis was performed at the end of each run to confirm the specificity of the reaction.

YB1(F):5'CGCAGTGTAGGAGATGGAGAG

YB1(R):5'GAACACCACCAGGACCTGTAA

ΔNp63 (F):5'GGTTGGCAAAATCCTGGAG

ΔNp63 (R):5'GGTTCGTGTACTGTGGCTCA

EGFR (F) :5'TTCCTCCCAGTGCCTGAA

EGFR (R):5'GGGTTCAGAGGCTGATTGTG

STAT3 (F) :5'CCTCTGCCGGAGAAACAG

STAT3 (R):5'CTGTCACTGTAGAGCTGATGGAG

GADD45A (F): 5' TTTGCAATATGACTTTGGAGGA

GADD45A (R): 5' CATCCCCCACCTTATCCAT

18S (F):5'TCGAGGCCCTGTAATTGGAA

18S (R):5'CTTTAATATACGCTATTGGAGCTG

Luciferase reporter assay

MDA-MB231 cells were co-transfected with ΔNp63α, ΔNp63α F518L and EGFR promoter-luciferase reporter vector. Transfections were performed in triplicate in each assay. At 24h after transfection, cells were harvested in 1x PLB buffer (Promega, Madison, USA) and luciferase activity was measured using Dual Luciferase Reporter system (Promega, Madison, USA) using pRL-TK activity as internal control. FireFly-derived luciferase activity was normalized for transfection efficiency. Successful transfection of p63 was confirmed by immunoblotting. The average values of the tested constructs were normalized to the activity of the empty construct.

Immunofluorescence and bright -field images acquisition

HaCaT cells (2.5 x 10^5) were plated in 35 mm dish, grown on micro cover glasses (BDH). At 24 hours after seeding, cells were washed with cold phosphate-buffered saline (PBS) and fixed with 4% paraformaldehyde (PFA) (Sigma-Aldrich, St. Louis, MO) for 15 min at 4°C. Cells were permeabilized with ice-cold 0.1% Triton X-100 for 10 min, washed with PBS and incubated with Thermo Scientific Hoechst 33342 (2'-[4-ethoxyphenyl]-5-[4-methyl-1-piperazinyl]-2,5'-bi-1H-benzimidazole trihydrochloride trihydrate) for 3 min. Images were digitally acquired at 470 nm using Nikon TE Eclipse 2000 microscope and processed using Adobe Photoshop software CS.

SCC022 cells (2.5 x 10^5) were plated in 35 mm dish and grown on micro cover glasses (BDH). At 24 hours after seeding, cells were transfected with scramble , YB-1 or p63 siRNA oligos. 48 hrs after silencing cells were washed with cold phosphate-buffered saline (PBS) and fixed with 4% paraformaldehyde (PFA) (Sigma-Aldrich, St. Louis, MO) for 15 min at 4°C. Cells were permeabilized with ice-cold 0.1% Triton X-100 for 10 min and then washed with PBS. P63 was detected using a 1:200 dilution of the monoclonal antibody D9 (Santa Cruz, Biotechnology Inc.,

CA, USA). YB-1 was detected using 1:100 dilution of the YB1 antibody (Ab12148). After extensive washing in PBS, the samples were incubated with Cy3-conjugated anti-mouse (red) and Cy5-conjugated anti-rabbit IgGs (green) at room temperature for 30 min. Cells were incubated with Hoechst 33342 (2'-[4-ethoxyphenyl]-5-[4-methyl-1-piperazinyl]-2,5'-bi-1H-benzimidazole trihydrochloride trihydrate) (Thermo Scientific) for 3 min. Images were digitally acquired and processed using Adobe Photoshop software CS.

Cell motility assay

SCC022 cells were cultured on 35-mm dishes (Corning, NY) at $2x10^4$ cells/dish density. ΔNp63α or YB1 transient silencing were performed as described above. After 24 h from silencing cell migration tests were performed via an Olympus IX81 inverted microscope equipped with a 10X objective and an integrated stage incubator (Okolab, Italy). Images of selected positions of the cell culture were collected in bright field for 16 h with 5-min frame intervals. All of the collected data were processed with the Olympus imaging software Cell^R. To quantify the cell speed (μm/min), time-lapse acquisitions were processed by the dedicated software add-in (TrackIT). The average speed per cell was calculated from the length of the path divided by time. An average number of 60 cells were analyzed for each condition.

Results

YB-1 knockdown in HaCaT cells

We have previously shown that ΔNp63α interacts with YB-1 in human squamous carcinoma cells and promotes accumulation of full length YB-1 protein (50 kDa) in the nuclear compartment (Di Costanzo et al., 2012). We first validated the interaction between YB-1 and ΔNp63α in non transformed HaCaT keratinocytes by co-immunoprecipitation assay (Supplementary Fig. 1). Then, we examined the effect of YB-1 silencing in mitotically active HaCaT keratinocytes. Interestingly, at 48 hrs of silencing we observed massive cell detachment (Figure 1A, upper panel) associated with a high proportion of condensed and fragmented nuclei (Figure 1A, lower panel). Western blot analysis showed a significant reduction of ΔNp63α protein level and PARP1 proteolytic cleavage (Figure 1B, left panel) indicating that YB-1 is critical for keratinocyte survival.

ΔNp63α is known to sustain survival in squamous cell carcinoma (Rocco et al., 2006, Hibi et al., 2000) and up-regulate cell adhesion-associated genes (Carrol et al., 2006). To rule out the possibility that YB-1 silencing induces cell death by merely reducing the level of ΔNp63α, we knocked down ΔNp63α expression in HaCaT cells by RNA interference. According to previous studies (Barbieri et al., 2006), we observed neither cell detachment (Figure 1A, upper panel) nor PARP1 activation (Figure 1B, right panel) clearly indicating that apoptosis, induced by YB-1 depletion, cannot be simply ascribed to the lack of ΔNp63α.

Next, we evaluated the level of ΔNp63α-specific transcript following YB-1 knockdown by Real Time quantitative PCR (RT-qPCR) and we found that it was drastically reduced (Figure 1C). After p63 silencing, instead, YB-1 transcript level was slightly enhanced (Figure 1D) while the mRNA of GADD45A, a gene induced by stressful conditions and used as control, was enhanced in both experiments (Figure 1C and D).

YB-1 knockdown in squamous carcinoma cells

Next, we used RNA interference to explore the function of YB-1 in squamous cell carcinoma (SCC). SCC011 and SCC022 are cell lines derived from cutaneous squamous carcinomas (Lefort et al., 2007). SCC022 are highly metastatic and, when subcutaneously injected in nude mice, form large tumors. SCC011 cells, instead, generate only keratin pearls (C. Missero, personal communication).

Similarly to what observed in HaCaT cells, YB1-depleted SCC011 cells detached from the plate generating abundant cellular debris (Figure 2A, upper panel) and exhibited a reduced level of ΔNp63α protein (Figure 2B). PARP1 cleavage was barely detectable (Figure 2B). On the other hand, we have previously demonstrated that p63 knockdown has no apparent effect on SCC011 cell viability (Di Costanzo et al., 2012).

Surprisingly, SCC022 cells looked healthy and tightly adherent to the plate after YB1 silencing (Figure 2A, lower panel). Moreover, as detected by immunoblot analysis, the expression level of ΔNp63α protein was significantly increased (Figure 2B). Interestingly, ΔNp63α transcript in SCC011 was reduced while in SCC022 it was 2.1-fold higher than control (Figure 2C).

Analysis of cell viability by the MTT assay showed that after 48 hrs of YB-1 knockdown the percentage of viability of SCC022 cells was 70% of the control, while it was reduced to 10% in HaCaT and SCC011 cells (Figure 4C).

We have also performed p63 knockdown in SCC022 cells and, as expected, we observed accumulation of YB-1 in the cytoplasm without any apparent effect on cell viability (Supplementary Fig. 2).

We also determined the influence of ΔNp63α or YB-1 silencing on SCC022 cell motility by time-lapse microscopy using siRNA-based silencing of endogenous proteins. According to our previous observations made on SCC011 cells (Di Costanzo et al., 2012) ΔNp63α silenced cells display

higher speeds ($p < 0.01$) than control cells. Conversely, SCC022 cell motility was unaffected by YB-1 depletion (Supplementary Fig. 3).

YB-1 silencing hyper-activates the PI3K/AKT signaling pathway in SCC022 cells

ΔNp63α is a target of the phosphoinositide-3-kinase (PI3K) pathway downstream of the Epidermal Growth Factor Receptor (Barbieri et al., 2003). We hypothesized an involvement of the PI3K/AKT pathway in the upregulation of ΔNp63α observed in SCC022 cells following YB-1 silencing, and we looked for changes in the phosphorylation status of $AKT_{Ser473.}$ Interestingly, unlike HaCaT and SCC011, SCC022 cells exhibited constitutive phosphorylation of AKT_{Ser473} which was reproducibly potentiated following YB-1 depletion (Figure 3A and B) suggesting that YB-1 expression restrains AKT activation. To corroborate this result, we treated YB1-silenced SCC022 cells with Ly294002, a highly selective PI3K inhibitor. Remarkably, Ly294002 treatment counteracted AKT hyperphosphorylation and the increase of ΔNp63α protein level in response to YB-1 silencing (Figure 3B). Moreover, it resulted in cell death and detachment (data not shown). Importantly, Ly294002 treatment alone had no apparent effect on ΔNp63α level and SCC022 cell viability (Figure 3B and data not shown). Quantification of ΔNp63α transcript in YB-1 depleted SCC022 cells, treated or not with LY294002, showed that the increase of ΔNp63α transcription was strictly dependent on the PI3K/AKT pathway (Figure 3B). Moreover, inhibition of the proteasome activity with MG132 did not significantly enhance ΔNp63α protein level in YB1-silenced SCC022 cells, thereby confirming that ΔNp63α up-regulation was almost exclusively at transcriptional level (Supplementary Fig. 4).

The PI3K/AKT signaling pathway is negatively regulated by the phosphatase and tensin homologue PTEN (Song et al., 2012). To further investigate on the ability of SCC022 cells to escape from death following YB-1 depletion, we compared the protein level of PTEN among HaCaT, SCC011

and SCC022 cell lines. Compared to HaCaT and SCC011 cells, the level of PTEN protein in SCC022 cells was very low, accounting for their high basal level of AKT_{Ser473} phosphorylation (Figure 3E). Furthermore, YB-1 silencing resulted in increased levels of cytoplasmic PTEN in HaCaT and SCC011 cells, while no effects on PTEN protein level was observed in YB-1 silenced SCC022 cells (Figure 3E).

Cross-talk of ΔNp63α and YB-1 with EGFR/STAT3 and PI3K/AKT signaling pathways

In pancreatic cancer cells, ΔNp63α expression was shown to induce the Epidermal Growth Factor Receptor (EGFR) (Danilov et al., 2011). As we observed a PI3K-dependent increase of ΔNp63α in SCC022 cells upon YB-1 silencing, we decided to evaluate the level of EGFR and its direct downstream target STAT3 in SCC022 cells upon YB-1 or ΔNp63α silencing. As shown in Figure 4, along with ΔNp63α, YB-1 depletion up-regulates EGFR and STAT3 both at protein (Figure 4A) and RNA level (Figure 4B). Real Time PCR assay in SCC022 cells clearly shows that YB-1 silencing results in about 2 and 3.5 fold induction of EGFR and STAT3 transcripts, respectively (Figure 4B). Following ΔNp63α silencing, instead, the expression of both EGFR and STAT3 was switched off although the level of YB-1 protein remained unaltered (Figure 4A). These results suggest that ΔNp63α is a major activator of the EGFR/STAT3 axis in squamous carcinoma cells. Accordingly, in SCC011 and HaCaT cells where YB-1 silencing reduces ΔNp63α, EGFR and STAT3 transcription was also reduced (Supplementary Fig. 5A and B).

To confirm the ability of ΔNp63α to regulate EGFR gene expression we performed transient transfection and luciferase reporter assays in MDA-MB231 breast cancer cells expressing no detectable p63. MDA-MB231 cells were transiently transfected with the EGFR promoter-luciferase vector and increasing amount of expression plasmid encoding wild type ΔNp63α or its mutant form bearing the F to L substitution at position 518 of the SAM domain. This mutant was

previously described to be transactivation defective (Radoja et al., 2007). Remarkably, wild type but not mutant ΔNp63α protein induced luciferase activity, in a dose-dependent manner (Figure 4C and D). Moreover, Western blot analysis of extracts from MDA-MB231 breast cancer cells transiently transfected with ΔNp63α showed induction of both EGFR and STAT3 endogenous proteins, confirming that EGFR and STAT3 expression are induced by ΔNp63α (Figure 4E).

DISCUSSION

YB-1 is a versatile protein associated with many malignancies. However, because of its multifunctional character, the role of YB-1 in neoplastic cell growth remains elusive (Bader et al., 2006).

Our previous (Di Costanzo et al., 2012) and present data show that ΔNp63α hyper-expression, as it occurs in squamous carcinoma cells, is associated with YB-1 nuclear localization where it is expected to play a pro-proliferative role. In the present manuscript we show that YB-1 depletion has a strong negative impact on cell survival of both immortalized HaCaT keratinocytes and non-metastatic SCC011 squamous carcinoma cells. Interestingly, in HaCaT and SCC011 cells, YB-1 knockdown causes a significant reduction of ΔNp63α transcription (Yang et al., 1999; Senoo et al., 2004). However, in HaCaT and SCC cells, ΔNp63α knockdown is not sufficient to trigger cell death thereby indicating that YB-1, in keratinocytes, plays additional p63-independent pro-survival functions.

Surprisingly, in highly metastatic SCC022 cells, YB-1 silencing does not result in cell death. Strikingly, in these cells, YB-1 silencing potentiates AKT activation suggesting that YB-1 can act as a negative regulator of the PI3K/AKT signaling pathway and its loss allows PI3K/AKT-dependent induction of pro-survival genes, including ΔNp63α. Interestingly, the low level of endogenous PTEN observed in SCC022 cells can likely explain the constitutive activation of the

PI3K/AKT pathway observed in this cell line. Remarkably, we have observed only in HaCaT and SCC011 cells a strong activation of PTEN in response to YB-1 depletion. In SCC022 cells, instead, where PI3K/AKT hyper-activation sustains ΔNp63α protein level, we did not observe any increase of PTEN after YB-1 depletion. However, at this stage, we can hypothesize that, in this cell line, PTEN cannot be up-regulated because of epigenetic or other inactivating mechanisms.

The evidence that PI3K/AKT hyperactivation in SCC022 cells is responsible for ΔNp63α transcriptional induction is in line with previous studies showing that ΔNp63α is positively regulated by the PI3K pathway (Barbieri et al., 2003). However, it is important to remind that ΔNp63α has been shown to repress the expression of PTEN (Leonard et al., 2011). Accordingly, in PTEN-proficient HaCaT and SCC011 cells, where YB-1 silencing causes a decrease of ΔNp63α, we observed an increase in the level of PTEN protein which is expected to restrain signaling by the PI3K pathway.

In summary, our results indicate that, being able to sustain ΔNp63α gene expression, YB-1 is part of a complex molecular network linking ΔNp63α to the PI3K/AKT/PTEN pathway and that establishment of a positive feedback loop coupling induction of ΔNp63α expression with PI3K/AKT activation may be a relevant step in progression of squamous carcinogenesis.

An important finding of our work is the observation that ΔNp63α controls the expression of the Epidermal Growth Factor Receptor switching-on the entire EGFR/STAT3 axis. Accordingly, in normal adult epidermis, the EGFR is predominantly expressed in basal keratinocytes and signaling events elicited by it are known to affect their proliferation and migration (Bito et al., 2011). ΔNp63α, therefore, represents an important molecular connection between YB-1, the PI3K/AKT and the EGFR/STAT3 signaling pathways. We can postulate that constitutive activation of PI3K/AKT, such as in PTEN-deficient cells, may likely cause persistence of ΔNp63α which can induce keratinocyte hyper-proliferation by impinging on the EGFR/STAT3 pathway. Interestingly,

in physiological conditions EGF-dependent and PI3K/AKT pathways are both required for efficient skin wound re-epithelialization (Haase et al., 2003). Moreover, EGFR/STAT3 inhibition was shown to be unable to induce apoptosis (Bito et al., 2003) thereby providing a plausible explanation of why ΔNp63α silencing alone was not sufficient to induce cell death in our experimental settings.

In summary, we have presented clear evidences to suggest that YB-1 can play a role in skin carcinogenesis. However, the molecular basis of cancer can widely vary and the ability of YB-1 to control multiple and overlapping pathways raises concerns about the consideration of YB-1 as an attractive target for therapy against metastatic squamous cancer. In particular, our results indicate that YB-1 knockdown in cells whose oncogenic transformation depends on PI3K/AKT constitutive activation is expected to enhance rather than arrest metastatic progression. Association of YB1-targeted therapy with drugs that target the PI3K and/or EGFR pathway should be evaluated as a valuable strategy to treat squamous carcinoma. *In vivo* experiments will help to clarify this relevant point.

Conflict of interest

The authors declare that they have no conflict of interest.

References

1. Amoresano A, Di Costanzo A, Leo G, Di Cunto F, La Mantia G, Guerrini L, Calabrò V. 2010. Identification of ΔNp63α Protein Interactions by Mass Spectrometry. J. Proteome Res. 9: 2042-48.
2. Bader AG. 2006. YB-1 activities in oncogenesis: transcription and translation. Curr Cancer Ther Rev . 2: 31–39.
3. Barbieri CE, Barton CE, Pietenpol JA. 2003. ΔNp63α expression is regulated by the phosphoinositide 3-kinase pathway. J Biol Chem; 278(51): 51408-51414.
4. Barbieri CE, Tang LJ, Brown KA, Pietenpol JA. 2006. Loss of p63 leads to increased cell migration and up-regulation of genes involved in invasion and metastasis. Cancer Research, 66: 7589- 7597.
5. Bito T, Sumita N, Ashida M, Budiyanto A, Ueda M, Ichihashi M, Tokura Y, Nishigori C. 2011. Inhibition of epidermal growth factor receptor and PI3K/AKT signaling suppresses cell proliferation and survival through regulation of Stat3 activation in human cutaneous cell carcinoma. Journal of Skin Cancer. doi:10.1155/2011/874571.
6. Carrol DK, Carrol JS, Leong CO, Cheng F, Brown M, Mills AA, Brugge JS, Ellisen LW 2006. p63 regulates an adhesion programme and cell survival in epithelial cells. Nat Cell Biol, 8(6): 551-561.
7. Danilov AV, Neupane D, Nagaraja AS, Feofanova E, Leigh AH, Di Renzo J., Kork M. 2011. DeltaNp63alpha-mediated induction of epidermal growth factor promotes pancreatic cancer cell growth and chemoresistence. Plos one: 6(10) e26815.
8. Di Costanzo A, Troiano A, Di Martino O, Cacace A, Natale CF, Ventre M, Netti P, Caserta S, Pollice A, La Mantia G, Calabrò V. 2012. The p63 protein isoforms ΔNp63α modulates

Y-box binding protein 1 in its subcellular distribution and regulation of cell survival and motility genes. J Biol Chem, 287(36):30170-80.

9. Eliseeva A, Kim ER, Guryanov SG, Ovchinnikov LP, Lyabin DN. 2011. Y-Box-Binding Protein 1 (YB-1) and its function. Biochemistry (Moscow), 76(13): 1402-1433.
10. Haase I, Evans R, Pofahl R, Watt FM. 2003. Regulation of keratinocytes shape, migration and wound epithelialization by IGF-1-and EGF-dependent signaling pathways. J Cell Sci . 116: 3227-3238.
11. Hibi K, Trink B, Patturajan M, Westra WH, Caballero OL, Hill DE, Ratoviski EA, Jen J, Sidransky D. 2000. Ais is an oncogene amplified in Squamous cell carcinoma. Proc. Natl. Acad. Sci. USA; 97: 5462-5467.
12. Leonard MK, Kommagani R, Payal V, Mayo LD, Shamma HN, Kadakia MP. 2011. ΔNp63α regulates keratinocytes proliferation by controlling PTEN expression and localization. Cell Death Differ. 18(12): 1924-1933.
13. Lefort K, Mandinova A, Ostano P, Kolev V, Calpini V, Kolfschoten I, Devgan V, Lieb J, Rafooul W, Hohl D, Neel V, Garlick J, Chiorino G, Dotto P. 2007. Notch 1 is a p53 target gene involved in human keratinocytes tumor suppression through negative regulation of ROCK1/2 and MRCKα kinases. Genes Dev, 21(5): 562-577.
14. Livak KJ, Schmittgen TD. 2011. Analysis of relative gene expression data using Real-Time Quantitative PCR and the $2^{-DDC}{}_{T}$ method. *Methods*. **25**: 402-408.
15. Lo Iacono M, Di Costanzo A, Calogero RA, Mansueto G, Saviozzi S, Crispi S, Pollice A, La Mantia G, Calabrò V. 2006. The Hay Wells Syndrome-Derived TAp63αQ540L Mutant has Impaired Transcriptional and Cell Growth Regulatory Activity. Cell Cycle, 5(1):78-87
16. Kolk A, Jubitz N, Mengele K, Mantwill K, Bissinger O, Schmitt M, Kremer M, Holm PS. 2011. Expression of Y-box-binding protein YB-1 allows stratification into long- and short-term survivors of head and neck cancer patients. Br J Cancer, 105(12):1864-1873.

17. Koster MI. 2010. p63 in skin development and ectodermal dysplasias. J Invest Dermatol; 130(10): 2352-2358.

18. Moll UM, Slade N. 2004. p63 and p73: roles in development and tumor formation. Mol Cancer Res; 2: 371-386.

19. Radoja N, Guerrini L, Lo Iacono N, Merlo GR, Costanzo A, Weinberg WC, La Mantia G, Calabro V, Morasso MI. 2007. Homeobox gene Dlx3 is regulated by p63 during ectoderm development: relevance in the pathogenesis of ectodermal dysplasias. Development 134(1): 13-18.

20. Ripamonti F, Albano L, Rossini A, Borrelli S, Fabris S, Mantovani R, Neri A, Balsari A, Magnifico A, Tagliabue E. 2013. EGFR through STAT3 modulates ΔNp63α expession to sustain tumor-initiating cell proliferation in squamous cell carcinomas. J Cell Physiol; 228(4): 871-8.

21. Rocco JW, Leong CO, Kuperwasser N, DeYoung MP, Ellisen LW. 2006. p63 mediates survival in squamous cell carcinoma by suppression of p73-dependent apoptosis. Cancer Cell; 9(1): 45-56.

22. Rossi M, De Simone M, Pollice A, Santoro R, La Mantia G, Guerrini L, Calabrò V. 2006. Itch/AIP4 associates with and promotes p63 protein degradation. Cell Cycle; 5(16):1816-22.

23. Schittek B, Psenner K, Sauer B, Meier F, Iftner T, Garbe C. 2007. The increased expression of Y box-binding protein 1 in melanoma stimulates proliferation and tumor invasion, antagonizes apoptosis and enhances chemoresistance. Int J Cancer, 120:2110–2118.

24. Senoo M, Manis JP, Alt FW, McKeon F. 2004. p63 and p73 are not required for the development and p53-dependent apoptosis of T cells. Cancer Cell; 6: 85-89.

25. Shiota M, Izumi H, Onitsuka T, Miyamoto N, Kashiwagi E, Kidani A, Yokomizo A, Naito S, Kohno K. 2008. Twist promotes tumor cell growth through YB-1 expression.Cancer Res, 68(1): 98-105.

26. Shiota M, Zoubeidi A, Kumano M, Beraldi E, Naito S, Nelson C, Sorensen P, Gleave M. 2011. Clusterin is a critical downstream mediator of stress-induced YB-1 transactivation in Prostate Cancer. Mol Cancer Res; 9:1755-1766.

27. Sinnberg T, Sauer B, Holm P, Spangler B, Kuphal S, Bosserhoff A, Schittek B. 2012. MAPK and PI3K/AKT mediated YB-1 activation promotes melanoma cell proliferation which is counteracted by an auto regulatory loop. Exp. Dermatol; 21(4):265-270.

28. Song MS, Salmena L, Pandolfi PP. 2012. The function and regulation of the PTEN tumor suppressor. Nature Reviews Molecular Cell Biology, 13: 283-296.

29. Sutherland BW, Kucab J, Wu J, Lee C, Cheang MC, Yorida E, Turbin D, Dedhar S, Nelson C, Pollak M, Leighton Grimes H, Miller K, Badve S, Huntsman D,Blake-Gilks C, Chen M, Pallen CJ, Dunn SE. 2005. AKT phosphorylates the Y-box binding protein 1 at Ser102 located in the cold shock domain and affects the anchorage-independent growth of breast cancer cells. Oncogene**,** 24(26):4281-4292.

30. To K, Fotovati A, Reipas KM, Jennifer HL, Hu K,Wang J, Astanehe A, Davies AH, Lee L, Stratford AL, Raouf A, Johnson P, Berquin IM, Royer HD, Eaves CJ, Dunn SE. 2010. YB-1 induces expression of CD44 and CD49f leading to enhanced self-renewal, mammosphere growth, and drug resistance. Cancer Res; 70(7): 2840-2851.

31. Toh S, Nakamura T, Ohga T, Koike K**,** Uchiumi T**,** Wada M**,** Kuwano M**,** Kohno K. 1998. Genomic organization of the human Y-box protein (YB-1) gene. *Gene*, 206:93 -97.

32. Uramoto H, Izumi H, Ise T, Tada M, Uchiumi T, Kuwano M, Yasumoto K, Keiko F, Kohno K. 2002. p73 interacts with c-Myc to regulate Y-box-binding protein-1 expression. J Biol Chem, 277: 31694-31702.

33. Yang A, Schweitzer R, Sun D, Kaghad M, Walker N, Bronson RT, Tabin C, Sharpe A, Caput D, Crum C, McKeon F. 1999. p63 is essential for regenerative proliferation in limb, craniofacial and epithelial development. Nature; 398: 714-71.

Figures Legend

Figure 1. YB-1 knockdown affects HaCaT cell survival. (**A) upper panel,** Phase-Contrast imaging and Hoechst staining (**lower panel**) showing HaCaT keratinocyte cells transfected with scrambled, YB-1 or p63 siRNA oligos. (**B**) Representative immunoblot analyses of HaCaT keratinocytes transfected with YB1 (**upper panel**), p63 (**lower panel**) or scrambled (siCtrl) siRNA oligos, respectively. 48 hours after silencing whole cell extracts were immunoblotted with YB-1, p63 and PARP antibodies. Actin was used as a loading control. Bar graphs are quantitative densitometric analyses of four indipendent Western blots. The blots were normalized to actin and the fold-changes of protein levels are reported in comparison to control (value set at 1.0). P-value <0.05 is represented by *; P-value <0.01 is represented by **. (**C**) Quantitative real-time PCR analysis of HaCaT keratinocytes transfected with scrambled or YB-1 siRNA oligos. GADD45A mRNA level was measured as a control. (**D**) Quantitative Real-time PCR analysis of HaCaT keratinocytes transfected with scrambled or p63 siRNA oligos. In both experiments data were analyzed according to the fold-changes compared to scrambled control (value set at 1.0) using the $2^{-\Delta\Delta Ct}$ method. P-value <0.05 is represented by *; P-value <0.01 is represented by **.

Figure 2. YB-1 knockdown in SCC011 and SCC022 squamous carcinoma cells. (A) Phase-contrast imaging showing SCC011 (**upper panel**) and SCC022 (**lower panel**) cells at 48 hours post-YB1 silencing. (**B**) Representative immunoblot analysis of SCC011 or SCC022 cells transfected with scrambled or YB-1 siRNA oligos. 48 hours after silencing whole cell lysates were immunoblotted with YB-1, p63 and PARP antibodies. GAPDH was used as a loading control. Bar graph is a quantitative densitometric analysis of four indipendent Western blots. The blots were normalized to GAPDH and the fold-changes of protein levels are reported in

comparison to control (value set at 1.0). P-value <0.05 is represented by *; P-value <0.01 is represented by **. (**C**) Quantitative Real-time PCR analysis of SCC011 (**left panel**) and SCC022 cells (**right panel**) transfected with scrambled or YB-1 siRNA oligos. Data were analyzed according to the fold-changes compared to scrambled control (value set at 1.0) using the $2^{-\Delta\Delta Ct}$ method. P-value <0.05 is represented by *; P-value <0.01 is represented by **. (**D**) Effect of YB1 silencing on the viability of HaCaT and SCC cells. Cell viability was assessed by MTT assay following 48 hours of YB-1 silencing. Data are represented as the mean +/- SD from three independent experiments. The asterisk indicates P-value<0.05.

Figure 3. YB-1 knockdown enhances pAKT^{S473} in SCC022 squamous carcinoma. (A) Immunoblot analysis of HaCaT, SCC011 and SCC022 cells transfected with scrambled or YB1-siRNA oligos. 48 hours after silencing whole cell extracts were immunoblotted with YB-1, pAKT^{S473} and AKT antibodies. Actin was used as a loading control. **(B)** SCC022 cells were transfected with scrambled or YB-1 siRNA oligos transfection. After 42 hrs cells were treated with LY294002 for 6 hrs. Whole cell extracts were analyzed by immunoblotting with YB-1, pAKT^{S473}, p63 and AKT antibodies. Actin was used as loading control. (**C**) Quantitative Real-time PCR of ΔNp63 mRNA levels. ΔNp63 mRNA levels were analyzed according to the fold-changes compared to scrambled control (value set at 1.0) using the $2^{-\Delta\Delta Ct}$ method. P-value < 0.05 is represented by *; P-value < 0.01 is represented by **. DMSO was used as control (**D**) Immunoblot analysis of HaCaT, SCC011 and SCC022 cells. Whole cell extracts were immunoblotted with, PTEN, pAKT^{S47} , and AKT antibodies. GAPDH was used as loading control. (**E**) Nuclear and cytoplasmic fractionation of extracts from control or YB-1 silenced HaCaT, SCC011 and SCC022 cells are shown in Figure 5A. Fractions were analysed by

immunoblotting with PTEN antibody. GAPDH and PARP were used as cytoplasmic and nuclear controls, respectively.

Figure 4. Cross-talk of ΔNp63α and YB-1 with EGFR/STAT3 pathway. (A) Immunoblot analysis of SCC022 cells transfected with scramble, YB-1 or p63 siRNA oligos. Whole cell extracts were immunoblotted with, YB-1, p63, EGFR, STAT3 antibodies. Actin was used as a loading control. **(B)** Quantitative Real-time PCR analysis of SCC022 cells transfected with scrambled or YB-1 siRNA oligos. YB-1, EGFR and STAT3 mRNA levels were analyzed according to the fold-changes compared to scrambled control (value set at 1.0) using the $2^{-\Delta\Delta Ct}$ method. P-value < 0.05 is represented by *; P-value < 0.01 is represented by **. **(C)** Luciferase assay of EGFR-promoter activity in MDA-MB231 cells. Cells were transiently transfected with 1μg of luciferase reporter plasmid and the indicated amounts of ΔNp63α or ΔNp63α F518L plasmids. Luciferase assay was performed at 48 hrs post-transfection. Values are the mean +/- SD of three independent experimental points. **(D)** Representative immunoblotting showing the level of ΔNp63α in transfected MDA-MB231 cell extracts used for the luciferase assay shown in 7C. GAPDH immunodetection was used as loading control. **(E)** MDA-MB231 cells were transfected with empty vector or ΔNp63α plasmids. At 24h post-transfection cells were harvested and whole cell extracts were analyzed by immunoblotting with p63, STAT3 and EGFR antibodies. Actin was used as a loading control.

Supplementary Figures

S1. YB-1 and ΔNp63α coimmunoprecipitation in HaCaT cells. (**A**) Extracts from HaCaT cells were immunoprecipitated with anti-p63 antibodies and the immunocomplexes were blotted and probed with anti-YB-1, as indicated. (**B**) Extracts from HaCaT cells were

immunoprecipitated with anti-YB-1 antibodies and the immunocomplexes were blotted and probed with anti-p63. Samples with no antibody (no Ab) or irrelevant α-mouse and α-rabbit antibodies were included as controls. (**C**) Immunoblot analysis of YB-1 level in HaCaT cells treated with proteasome inhibitor MG132 for 6h (5μM final concentration). 36kDa and 43kDa YB-1 forms are reduced with concomitant accumulation of full-length YB-1 50kDa band showing the identity of YB-1 bands.

S2. **YB-1 and p63 knockdown in SCC022 cells. (A)** Immunofluorescence assay in SCC022 cells transfected with scrambled, YB-1 or p63 siRNA oligos. YB1 was detected using anti-YB-1 and secondary anti-rabbit Cy5-conjugated (green) antibodies. p63 was detected using anti-p63 and secondary anti-mouse Cy3-conjugated (red) antibodies. Hoechst was used to stain nuclei**. (B)** (upper panel**)** SCC022 cells were incubated with normal mouse serum and secondary anti-mouse Cy3-conjugated (red) antibodies; (lower panel) SCC022 cells were incubated with normal rabbit serum and secondary anti-rabbit Cy5-conjugated (green) antibodies.

S3. Effect of p63 and YB-1 silencing on SCC022 cells migration speed. (A) Motility assay on SCC022 cells after transient silencing of p63 and YB-1 performed by time-lapse microscopy. After 24 h of incubation with siRNA oligos, cell migration assay was performed. Averaged cell speeds after 16 h of observation are reported. Horizontal lines and boxes and whiskers represent the medians, 25th/75th, and 5th/95th percentile, respectively. P-value < 0.01 is represented by **. Only statistically different doubles are marked. (**B**) Immunoblot analysis of ΔNp63α and YB-1 protein levels in SCC022 cells after 40 h of ΔNp63α or YB-1 silencing and used in cell migration assay. Cell extracts were blotted and probed with anti-p63 or anti-YB-1 antibodies. GAPDH was used as a loading control. ΔNp63α protein band was almost undetectable while YB-1 protein was reduced to 40%, as assed by densitometric scanning.

S4. Proteasome activity is not involved in ΔNp63α up-regulation upon YB-1 silencing. Immunoblot analysis of SCC022 cells transfected with scrambled or YB1-siRNA oligos and treated with MG132 (6 hrs) after 42 hours of YB-1 silencing cells. Whole cell extracts were immunoblotted with YB-1 and p63 antibodies. Actin was used as loading control.

S5. Effect of YB-1 silencing on EGFR/STAT3 mRNA levels in SCC011 and HaCaT cells. Quantitative Real-time PCR analysis of **(A)** SCC011 cells and **(B)** HaCaT cells transfected with scrambled or YB-1 siRNA oligos. YB-1, EGFR and STAT3 mRNA levels were analyzed according to the fold-changes compared to scrambled control (value set at 1.0) using the $2^{-\Delta\Delta Ct}$ method. P-value < 0.05 is represented by *; P-value < 0.01 is represented by **.

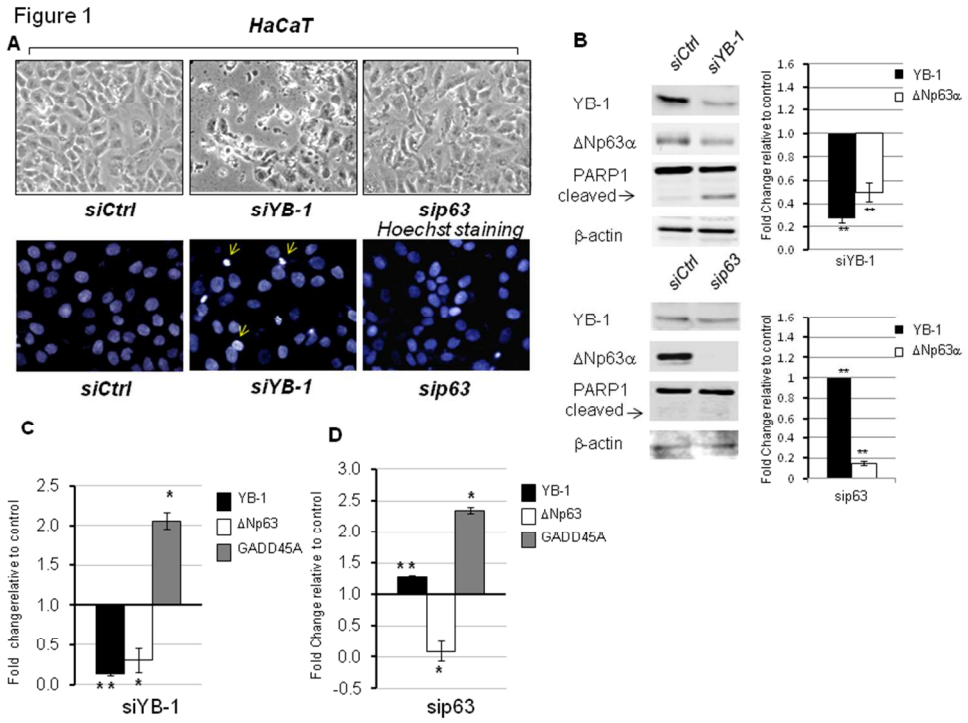

YB-1 knockdown affects HaCaT cell survival. (A) upper panel, Phase-Contrast imaging and Hoechst staining (lower panel) showing HaCaT keratinocyte cells transfected with scrambled, YB-1 or p63 siRNA oligos. (B) Representative immunoblot analyses of HaCaT keratinocytes transfected with YB1 (upper panel), p63 (lower panel) or scrambled (siCtrl) siRNA oligos, respectively. 48 hours after silencing whole cell extracts were immunoblotted with YB-1, p63 and PARP antibodies. Actin was used as a loading control. Bar graphs are quantitative densitometric analyses of four indipendent Western blots. The blots were normalized to actin and the fold-changes of protein levels are reported in comparison to control (value set at 1.0). P-value <0.05 is represented by *; P-value <0.01 is represented by **. (C) Quantitative real-time PCR analysis of HaCaT keratinocytes transfected with scrambled or YB-1 siRNA oligos. GADD45A mRNA level was measured as a control. (D) Quantitative Real-time PCR analysis of HaCaT keratinocytes transfected with scrambled or p63 siRNA oligos. In both experiments data were analyzed according to the fold-changes compared to scrambled control (value set at 1.0) using the 2-ΔΔCt method. P-value <0.05 is represented by *; P-value <0.01 is represented by **.
254x190mm (96 x 96 DPI)

Figure 2

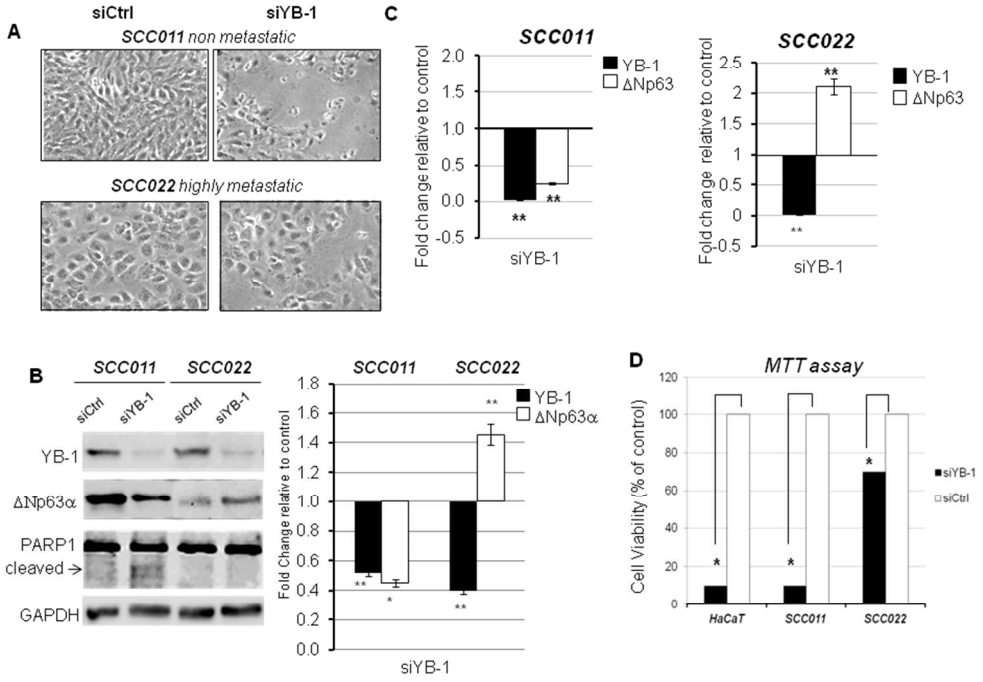

YB-1 knockdown in SCC011 and SCC022 squamous carcinoma cells. (A) Phase-contrast imaging showing SCC011 (upper panel) and SCC022 (lower panel) cells at 48 hours post-YB1 silencing. (B) Representative immunoblot analysis of SCC011 or SCC022 cells transfected with scrambled or YB-1 siRNA oligos. 48 hours after silencing whole cell lysates were immunoblotted with YB-1, p63 and PARP antibodies. GAPDH was used as a loading control. Bar graph is a quantitative densitometric analysis of four indipendent Western blots. The blots were normalized to GAPDH and the fold-changes of protein levels are reported in comparison to control (value set at 1.0). P-value <0.05 is represented by *; P-value <0.01 is represented by **. (C) Quantitative Real-time PCR analysis of SCC011 (left panel) and SCC022 cells (right panel) transfected with scrambled or YB-1 siRNA oligos. Data were analyzed according to the fold-changes compared to scrambled control (value set at 1.0) using the 2-ΔΔCt method. P-value <0.05 is represented by *; P-value <0.01 is represented by **. (D) Effect of YB1 silencing on the viability of HaCaT and SCC cells. Cell viability was assessed by MTT assay following 48 hours of YB-1 silencing. Data are represented as the mean +/- SD from three independent experiments. The asterisk indicates P-value<0.05.
254x190mm (96 x 96 DPI)

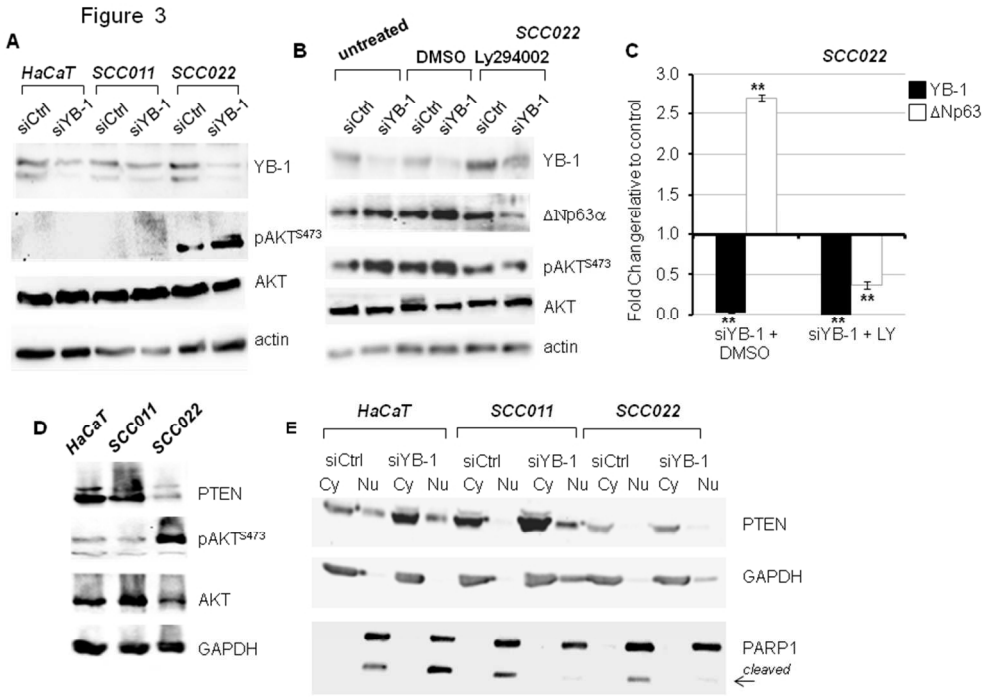

YB-1 knockdown enhances pAKTS473 in SCC022 squamous carcinoma. (A) Immunoblot analysis of HaCaT, SCC011 and SCC022 cells transfected with scrambled or YB1-siRNA oligos. 48 hours after silencing whole cell extracts were immunoblotted with YB-1, pAKTS473 and AKT antibodies. Actin was used as a loading control. (B) SCC022 cells were transfected with scrambled or YB-1 siRNA oligos transfection. After 42 hrs cells were treated with LY294002 for 6 hrs. Whole cell extracts were analyzed by immunoblotting with YB-1, pAKTS473, p63 and AKT antibodies. Actin was used as loading control. (C) Quantitative Real-time PCR of ΔNp63 mRNA levels. ΔNp63 mRNA levels were analyzed according to the fold-changes compared to scrambled control (value set at 1.0) using the 2-ΔΔCt method. P-value < 0.05 is represented by *; P-value < 0.01 is represented by **. DMSO was used as control (D) Immunoblot analysis of HaCaT, SCC011 and SCC022 cells. Whole cell extracts were immunoblotted with, PTEN, pAKTS47 , and AKT antibodies. GAPDH was used as loading control. (E) Nuclear and cytoplasmic fractionation of extracts from control or YB-1 silenced HaCaT, SCC011 and SCC022 cells are shown in Figure 5A. Fractions were analysed by immunoblotting with PTEN antibody. GAPDH and PARP were used as cytoplasmic and nuclear controls, respectively.

254x190mm (96 x 96 DPI)

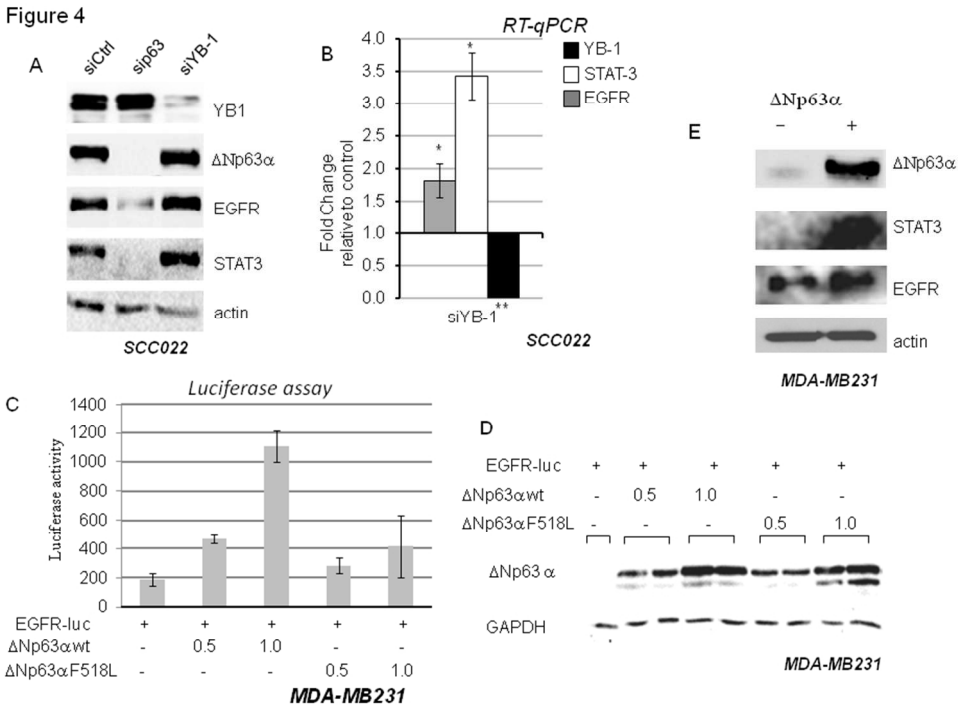

Cross-talk of ΔNp63α and YB-1 with EGFR/STAT3 pathway. (A) Immunoblot analysis of SCC022 cells transfected with scramble, YB-1 or p63 siRNA oligos. Whole cell extracts were immunoblotted with, YB-1, p63, EGFR, STAT3 antibodies. Actin was used as a loading control. (B) Quantitative Real-time PCR analysis of SCC022 cells transfected with scrambled or YB-1 siRNA oligos. YB-1, EGFR and STAT3 mRNA levels were analyzed according to the fold-changes compared to scrambled control (value set at 1.0) using the 2-ΔΔCt method. P-value < 0.05 is represented by *; P-value < 0.01 is represented by **. (C) Luciferase assay of EGFR-promoter activity in MDA-MB231 cells. Cells were transiently transfected with 1μg of luciferase reporter plasmid and the indicated amounts of ΔNp63α or ΔNp63α F518L plasmids. Luciferase assay was performed at 48 hrs post-transfection. Values are the mean +/- SD of three independent experimental points. (D) Representative immunoblotting showing the level of ΔNp63α in transfected MDA-MB231 cell extracts used for the luciferase assay shown in 7C. GAPDH immunodetection was used as loading control. (E) MDA-MB231 cells were transfected with empty vector or ΔNp63α plasmids. At 24h post-transfection cells were harvested and whole cell extracts were analyzed by immunoblotting with p63, STAT3 and EGFR antibodies. Actin was used as a loading control.
254x190mm (96 x 96 DPI)